J|A|C|S
COMMUNICATIONS

Published on Web 08/29/2002

Single-Crystalline Star-Shaped Nanocrystals and Their Evolution: Programming the Geometry of Nano-Building Blocks

Sang-Min Lee,[†] Young-wook Jun,[‡] Sung-Nam Cho,[†] and Jinwoo Cheon*[,†]

Department of Chemistry, Yonsei University, Seoul 120-749, Korea, and Korea Advanced Institute of Science and Technology, Taejon 305-701, Korea

Received May 6, 2002

The architectural control of nano-building blocks with well-defined shapes remains a key obstacle to overcome in the discovery of novel nanoscale properties and is essential for the success of "bottom-up" approaches toward future nanodevices.[1] Although excellent studies on novel colloidal nanocrystals such as rods,[2−4] cubes,[5] and prisms[6] have been recently carried out, the ability to understand and predict the final architectures of building blocks is still limited. If the shape-guiding processes in these building blocks are understood, it could be possible to program the system to yield the final building blocks with desired shape and crystallinity. Here, as a model study for the shape-guiding strategy, we present a rational synthetic scheme that yields novel architectures of semiconductor nanocrystals. We are, in particular, interested in PbS system which is an attractive semiconductor with a narrow band gap energy of 0.41 eV and potential applications such as near-IR communication and switches. While previous works of CdSe rods by Alivisatos et al.[2] were possible through the inherently anisotropic (*c*-axis) nature of its hexagonal cell structure and those of Pt nanocrystals by El-Sayed et al.[5] were limited to shapes of cubes and tetrahedrons, we demonstrate in this study that a series of shape evolutions ranging from anisotropic (i.e., rods) to isotropic (i.e., cubes) forms is possible even in highly symmetric rock-salt phased semiconductors. Specifically, the shapes of PbS nanocrystals studied are unusual and evolve from metastable one-dimensional (1-D) rod-based structures through star-shaped structures as a transient species to stable truncated octahedron and cubes. Simultaneously, we elucidate the specific role of important growth parameters for shape determinations.

Well defined, but structurally unprecedented, star-shaped PbS nanocrystals (Figure 1a) were synthesized from the thermal decomposition of a molecular precursor, $Pb(S_2CNEt_2)_2$, which was injected into a hot phenyl ether solvent at ∼230 °C containing the capping molecule, dodecanethiol (DT). TEM zone axis analyses show a clear view of its three-dimesional (3-D) stereographic-structure (Figure 1a−d).[7] It possesses well-defined geometry and rock-salt phased single-crystallinity.[8] As the zone axis is changed from [111] to [110], [112], and [100] by tilting the sample holder, the structural images and electron diffraction patterns simultaneously change. A star shape is only seen through the zone axis of [111] since it is in fact a 2-D projection of a 3-D real structure with truncated octahedron core and six symmetric horns in the [100] direction.

In addition, we found that shape evolutions of a variety of novel structures including 1-D rod-based structures, highly faceted star shapes, truncated octahedrons and cubes are also possible as a result of adjusting the key growth parameters.

When growth temperature was fixed at ∼140 °C with a reaction time of ∼5 min. in the presence of DT, a variety of rod-based nanocrystals (Figure 2a) including tadpole-shaped monorods (∼20%,

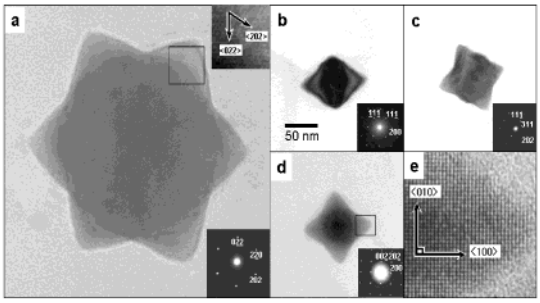

Figure 1. (a) TEM image of star-shaped PbS nanocrystals synthesized at 230 °C. (Inset) HRTEM imasge of lattice fringes with zone azis of [111]. (b−d) TEM images and electron diffraction patterns with zone axis of (b) [110], (c) [112], (d) [100], respectively. (e) HRTEM image of zoomed fringes with zone axis of [100].

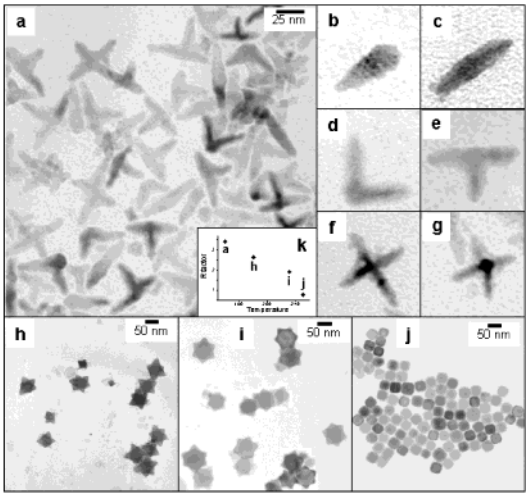

Figure 2. TEM images of rod-based multipods, star-shaped nanocrystals, and truncated octahedron. (a) TEM image of rod-based PbS multipods synthesized at 140 °C. (b) Tadpole-shaped monopod, (c) I-shaped bipod, (d) L-shaped bipod, (e) T-shaped tripod, (f) cross-shaped tetrapod, and (g) pentapod. (h) At 180 °C, star-shaped nanocrystals, (i) at 230 °C, more rounded star shapes, and (j) at 250 °C, truncated octahedrons are observed. (k) Temperature dependence of *R* factor.

Figure 2b), I-shaped bipods (∼12%, Figure 2c), L-shaped bipods (∼8%, Figure 2d), T-shaped tripods (∼34%, Figure 2e), cross-shaped tetrapods (∼14%, Figure 2f), and pentapods (∼2%, Figure 2g) were obtained. The widths of these nanorods are similar (9.6 nm, $\sigma = \sim 12\%$). As separate experiments, under conditions of fixed growth time (5 min) and precursor concentration, varying the growth temperature resulted in further shape evolution (Figure 2h−j), respectively. When the temperature was increased to ∼180 °C, highly faceted star-shaped nanocrystals with a size of ∼52 nm ($\sigma = \sim 12\%$) were obtained (Figure 2h). Increasing it even further (∼230 °C) produced rather rounded, but well-defined, star-shaped

* Corresponding author. E-mail: jcheon@alchemy.yonsei.ac.kr.
[†] Yonsei University.
[‡] Korea Advanced Institute of Science and Technology.

10.1021/ja026805j CCC: $22.00

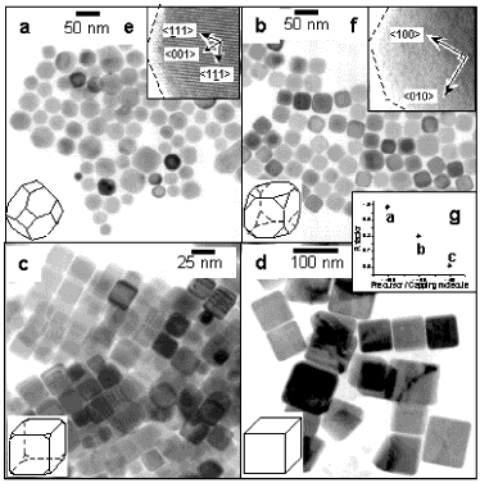

Figure 3. TEM images of PbS nanocrystals synthesized at 250 °C. (a−c) Dodecanethiol (DT) capping molecular molecular system. The ratio of precursor to capping molecules is (a) 1/400, (b) 1/100, and (c) 1/50, respectively. (d) Dodecylamine (DDA) capping molecular system with the ratio of precursor to capping molecule of 1/100. (e) HRTEM image of a round truncated octahedron with zone axis of [110], and (f) a truncated octahedron with zone axis of [100]. (g) *R* factor depends on the relative ratio of precursor to capping molecules.

crystals (∼57 nm, $\sigma = \sim 10\%$) (Figures 1 and 2i). Finally, at ∼250 °C the formation of truncated octahedrons (i.e., tetradecahedron) with a diameter of 35 nm ($\sigma = \sim 9\%$) was observed (Figure 2j). The decrease in *R* factor (r_{100}/r_{111}, the ratio of the central distance of the {100} faces to that of the {111} faces) from 3.4 to 2.7, 1.9, and 0.8 is observed as the temperature is increased (Figure 2k).

At high ratios of dodecanethiol (DT) concentration relative to that of the precursor (molar ratio of 400:1), nearly spherically shaped tetradecahedron nanocrystals truncated in the [111] direction were formed (Figure 3a). As the relative concentration of the capping molecule was decreased, the shape of the nanocrystals gradually changed from round to cubic (Figure 3b,c). Accordingly, the *R* factor gradually decreased from 0.98 to 0.79, and finally to 0.60 (Figure 3g), revealing that a higher concentration of DT in fact blocks growth on the {111} faces and enhances growth on the {100} faces.

Use of dodecylamine (DDA) instead of DT resulted in exclusive formation of the cube-shaped nanocrystals (Figure 3d). Since DDA is a weakly binding ligand to the PbS crystals (i.e., much weaker than thiol-to-Pb metal bonding), the growth of PbS crystals is enhanced. Since the formation of the 2-D nuclei on {111} faces has a low activation energy in weakly binding capping molecules,[9] growth on the {111} faces is now favored ($R = 0.58$), and formation of rather large (∼90 nm) PbS crystals with a perfect cubic shape is facilitated.

The structural aspects were examined to provide insight into the shaping guiding processes. HRTEM analyses show that a tadpole-shaped monorod has single-crystalline rock-salt structure. The hexagonal shape with four {111} and two {100} faces, which is identical to the [110] projection of a truncated octahedron,[10] is observed as the head of the rod.[11] The long axis of the rod is parallel to the [100] direction. This result indicates that truncated octahedral seed formation followed by preferential growth on the (100) face results in the formation of a tapered monorod with a large rounded head. Similar insight can also be obtained from a cross-shaped tetrapod. It also has rock salt structure with a separation angle of ∼90° between the pods of the cross and with an interplanar distance between [100] and [010] directions parallel to the two perpendicular axes of 0.29 nm. An octagonal shape (i.e., [001] projection of a truncated octahedron) is observed in the central junction of the cross, and the formation of the cross is possible through the preferential growth on the four opposite faces of the {100} faces of the truncated octahedral seeds.[11]

Our systematic studies of varying growth parameters in conjunction with detailed structural studies can provide a map of the shape-evolution process. Low-temperature conditions (∼140 °C) with a high flux of monomers results in kinetically controlled growth, and growth on the {100} faces is favored. As the growth rate is accelerated by increasing the temperature (∼180 °C), the enhanced growth rate on the {100} faces induces the shrinking of the six {100} faces into sharp triangular corners which finally results in star-shaped nanocrystals. After further increasing the growth temperature (∼230 °C), the relative growth rate difference between the surfaces with low activation barrier ({100} faces) and with high activation barrier ({111} faces) diminishes. Therefore, growth on the (111) surfaces as well as the (100) surfaces induces a star shape with a relatively round central body (Figure 1). These temperature-dependent growth rate changes of each surface are directly observed in the plot of *R* factor against temperature (Figure 2k). However, when excess thermal energy is supplied by either utilizing much higher growth temperatures (∼250 °C) or heating for extended periods of time (∼10 min), the growth process appears to shift into the thermodynamic regime, and the more thermodynamically stable cube shape with marginal truncation on its corners (i.e., tetradecahedron) is favored.

Throughout these analyses, we have discovered critical factors for determining the architectural features of the PbS nanocrystals. The initial injection of molecular precursor into hot solvent immediately results in the formation of truncated octahedron-shaped nuclei terminated by two characteristic faces: {100} faces with high surface energy and {111} faces with low surface energy in the presence of strong adsorbent. Several growth variables discussed in this work are now responsible for balancing the relative growth rates between these crystallographic faces and ultimately determine the final geometry of the PbS nanocrystals. In principle, through programming these growth parameters in the initial synthetic scheme, the desired architecture of building blocks including transient species such as star-shaped nanocrystals can be consistently obtained. These types of mechanistic studies may be the basis for controlling the geometries of a wide range of novel nanocrystals.

Acknowledgment. This work was supported by KOSEF (1999-1-122-001-5, 2000-6-122-03-2).

Supporting Information Available: Enlarged Figures 1−3, HR-TEM images of tadpole- and cross-shaped multipods, XRD analysis and detailed experimental procedure for PbS nanocrystals (PDF). This material is available free of charge via the Internet at http://pubs.acs.org.

References

(1) (a) Alivisatos, A. P. *J. Phys. Chem.* **1996**, *100*, 13226. (b) Hu, J.; Odom, T. W.; Lieber, C. M. *Acc. Chem. Res.* **1999**, *32*, 435. (c) Markovich, G.; Collier, C. P.; Henrichs, S. E.; Remacle, F.; Levine, R. D.; Heath, J. R. *Acc. Chem. Res.* **1999**, *32*, 415.
(2) (a) Peng, X.; Manna, L.; Yang, W.; Wickham, J.; Scher, E.; Kadavanich, A.; Alivisatos, A. P. *Nature* **2000**, *404*, 59. (b) Manna, L.; Scher, E. C.; Alivisatos, A. P. *J. Am. Chem. Soc.* **2000**, *122*, 12700.
(3) Puntes, V. F.; Krishnan, K. M.; Alivisatos, A. P. *Science* **2001**, *291*, 2115.
(4) (a) Peng, Z. A.; Peng, X. *J. Am. Chem. Soc.* **2001**, *123*, 1389. (b) Jun, Y.; Lee, S.-M.; Kang, N.-J.; Cheon, J. *J. Am. Chem. Soc.* **2001**, *123*, 5150. (c) Jun, Y.; Jung, Y.; Cheon, J. *J. Am. Chem. Soc.* **2002**, *124*, 615.
(5) Ahmadi, T. S.; Wang, Z. L.; Green, T. C.; Henglein, A.; El-Sayed, M. A. *Science* **1996**, *272*, 1924.
(6) Jin, R.; Cao, Y.; Mirkin, C. A.; Kelly, K. A.; Schatz, G. C.; Zheng, J. G. *Science* **2001**, *294*, 1901.
(7) TEM measurements are carried out on an EM912 Omega (KBSI).
(8) It is also confirmed by XRD analysis. See Supporting Information.
(9) Sugimoto, T. *J. Colloid Interface Sci.* **1983**, *91*, 51.
(10) Wang, Z. L. *J. Phys. Chem. B.* **2000**, *104*, 1153.
(11) See Supporting Information for more details.

JA026805J